Lifetimes of Metastable CO and N_2 Molecules*

Walter L. Borst† and Edward C. Zipf

Department of Physics, University of Pittsburgh, Pittsburgh, Pennsylvania 15213

(Received 21 October 1970)

The average lifetime of metastable CO molecules in the $a^3\Pi$ state excited by electron impact at 7.5 eV at room temperature was found to be about 1 msec. Lifetimes of metastable N_2 molecules in the $a^1\Pi_g$ and $E^3\Sigma_g^+$ states were found to be 115 ± 20 and 190 ± 30 μsec, respectively. There was evidence for at least one higher-lying metastable state of CO at about 10eV having a lifetime of about 0.1 msec. The lifetimes were obtained in a time-of-flight experiment and deduced from the measurements without resorting to analytic expressions of the time-of-flight distribution. The observed time-of-flight distributions were essentially Maxwellian. A diffuse-gas source operated at pressures in the 10^{-4}-Torr range was used. Effects due to metastable recoil, uv photons from metastable decay, and metastable wall collisions were carefully examined and found to be negligible under most conditions. Metastable excitation functions were obtained using a low-energy high-resolution electron gun.

I. INTRODUCTION

Metastable carbon monoxide and nitrogen molecules are of considerable interest in the atmospheres of Mars and Earth where they play an important role in atmospheric emission and collision processes. Their lifetimes enter into the evaluation of laboratory measurements of reactions involving these excited molecules, in particular cross-section measurements for electron-impact excitation. In the latter measurements, metastable lifetimes need to be known since the excited molecules may collide with other molecules or the chamber walls before they radiate. We have therefore attempted to measure metastable lifetimes of some important molecular states of N_2 and CO. Besides being of interest in themselves, the N_2 measurements served as a means of comparison in the determination of CO metastable lifetimes and as a check of our experimental method. We have used a time-of-flight technique to measure metastable lifetimes. This, together with the use of a high-resolution electron gun which we operated near the excitation thresholds, enabled us to separate different metastable states from each other. Care had to be exercised in order to determine the proper shape of the time-of-flight distributions. In doing this it was necessary to consider metastable-recoil problems, uv photons from metastable decay, and wall collisions of metastables. It was found that with the use of diffuse-gas sources and relatively large detector solid angles, the measured time-of-flight distributions were Maxwellian to a high degree of accuracy (except of course for factors accounting for the metastable decay). The primary lifetime values were obtained by comparing the time-of-flight distribution for the metastable state in question with that for the $A^3\Sigma_u^+$ state of N_2 which, for the purposes of our experiment, showed no significant decay. As a result of this work, we feel that the technique described in this paper can yield lifetime values in the range from below 10^{-4} sec to larger than 10^{-2} sec. It appears further that the technique employed in this work has distinct advantages over other methods where the distance between metastable detector and excitation region is varied. In the present time-of-flight experiment, the detector position is fixed. Thus, it is simpler to determine the detector-excitation chamber geometry and momentum-recoil problems. The use of a diffuse-gas source further simplified the data analysis. The metastable molecules were obtained by monitoring Auger secondary electrons from a surface detector. Obviously, the individual vibrational and rotational levels of a given metastable state could not be distinguished. We therefore obtained an average lifetime for the $a^3\Pi$ state of CO for which the individual vibrational-rotational transitions may involve different lifetimes. Nonetheless, this average lifetime for CO metastables is judged to represent useful information because it is this effective lifetime which enters in the analysis of laboratory cross-section measurements and collision processes in the Martian atmosphere involving electrons.

II. EXPERIMENTAL

A schematic diagram of the apparatus used in these experiments is shown in Fig. 1. The basic elements included a periodically pulsed system for metastable production, a metastable detector, and a digital processing system. Details of these sys-

tems are described below.

The metastable production and detection systems were housed in an ultrahigh-vacuum chamber. Gas was admitted into the collision chamber by means of a gas-handling system incorporating automatic pressure control. The gas pressure was about 10^{-4} Torr and approximately uniform within the collision chamber. (The background pressure was about 1×10^{-7} Torr.) Under these conditions the collision chamber closely approximated a diffuse-gas source. This was an advantage in the present measurements when compared with the use of a directed gas beam since momentum-recoil problems were minimized.

A. Metastable Production

Metastable CO and N_2 molecules were produced by electron impact in the energy range from threshold to about 50 eV. The electron gun used in these experiments was similar to a gun described previously.[1] Because of the required relatively high beam current ($10\mu A$) and good energy resolution [0.3 eV full width at half-maximum (FWHM)], the gun was not operated in the retarding-potential-difference (RPD) mode. A magnetic field of about 150 G collimated the electron beam.[2] The electron gun was pulsed at the retarding plate to inject bursts of electrons into the collision chamber. This enabled one to measure the arrival time of the metastable molecules at the detector, and thus we obtained time-of-flight distributions from which the metastable lifetimes could be extracted (see Sec. III). Beam pulses were typically 1–10 μsec wide with repetition rates of about 10^3 pulses/sec. The duty cycle of the gun was thus varied from 0.1 to 1%. The equipment for pulsing the gun consisted of a time-mark generator, discriminator, gate generator, and beam pulser; these are shown in Fig. 1.

Thermal metastable molecules produced during the on time of the electron beam traveled isotropically in all directions because of the diffuse nature of the gas souce (collision chamber); this assumes negligible momentum recoil (see below). A small fraction of these metastables was collimated and entered the metastable detector. The arrival times of these metastables at the detector, after the beam pulse and the time-of-flight spectra, were thus obtained (see Figs. 2 and 3).

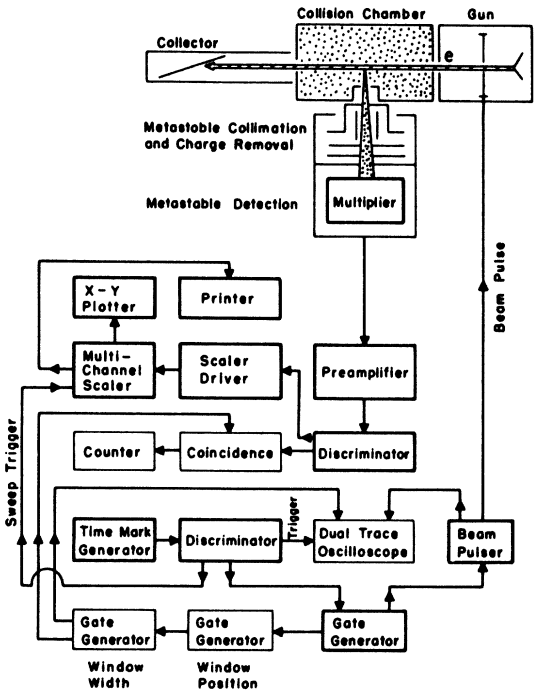

FIG. 1. Schematic diagram of experimental system. The boxes drawn with heavy lines (e.g., multichannel scaler) were used almost exclusively for measuring time-of-flight distributions. The boxes drawn with thin lines (e.g., coincidence) represent a single-channel analyzer of variable channel width and position which was used to check the multiscaling method and to obtain metastable excitation functions (see text).

B. Metastable Detection

After collimation and charged-particle removal, metastable particles impinged upon the dynode of a nude Cu-Be electron multiplier, from which they could liberate secondary electrons via the Auger process.[3] All metastable states of N_2 and CO have excitation energies greater than the work function of Cu-Be ($\phi\simeq4$ eV) and therefore contributed to the signal; the secondary yield of course was different for each state. Metastable detection by means of secondary electron emission from metal surfaces is a very convenient technique and has been used previously with good results.[1,4]

The solid angle subtended by the multiplier entrance aperture was about 0.05 sr. The effective scattering length in the collision chamber was about 0.5 cm. The distance between the center of the collision chamber and the detector was 6.4 cm. This resulted in transit times of the order of 100 μsec for thermal N_2 and CO molecules (see Figs. 2 and 3).

Total counting rates at the detector, summing over all metastable arrival times, were of the order of 10–100 counts/sec. The background counting rate was about 0.05 counts/sec. The low signal levels encountered clearly indicate the advantage of multiscaling techniques in order to obtain good time resolution as well as good statistics in the time-of-flight spectra.

C. Data Processing

Time-of-flight spectra of metastable molecules

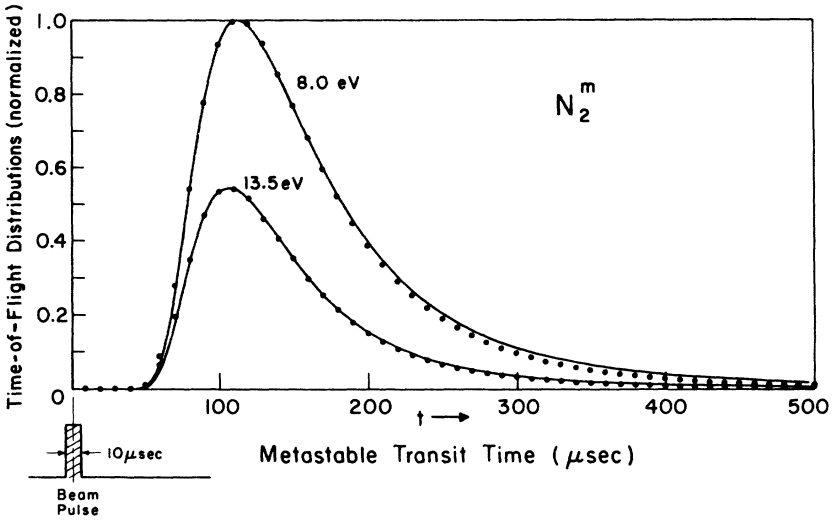

FIG. 2. Normalized time-of-flight distributions of metastable N_2 molecules. The solid dots represent experimental points. The solid lines represent Maxwellian distributions (without decay for the 8-eV data and with decay for the 13.5-eV data) fitted to the data (see text). The 8.0-eV data contain only metastables in the $A^3\Sigma_u^+$ state and thus show no metastable decay for the purposes of this experiment. The 13.5-eV data contain metastables in both the $A^3\Sigma_u^+$ and $a^1\Pi_g$ states. The normalization for the 13.5-eV curve is such that without decay of the $a^1\Pi_g$ state, the maximum of the curve would coincide with that for the 8.0-eV curve. It is seen that the decay of $a^1\Pi_g$ metastables shifts the maximum towards shorter transit times and causes a faster decline in the curve.

(Figs. 2 and 3) were obtained with a multichannel-analyzer system operated in the multiscaling mode. The components used in this mode are shown as boxes with heavy lines in Fig. 1. The memory cycle of the analyzer was triggered at the same time the electron beam was turned on. The channel address of the memory was either internally or externally programmed. Time-of-flight distributions were plotted on an X-Y plotter, printed out on paper, and also punched on tape. The total accumulation time for each distribution was about 5 h. This corresponded to about 10^7 sweeps (beam pulses). The total number of counts per channel was of the order of 10^4. For the time-of-flight distributions in Figs. 2 and 3 the dwell time per channel was 10 μsec.

It is seen in these figures that the fastest metastable started arriving at the detector at about 50 μsec after the beam pulse. The time-of-flight distributions reached a maximum about 100 μsec after the beam pulse was cut off. The time spacing between beam pulses was several milliseconds in order to allow the time-of-flight distributions to decay completely, thereby avoiding pile-up effects. Metastable lifetimes were inferred from the shape of the time-of-flight distributions using the known shape for infinitely long-lived metastables. The method used in obtaining the lifetimes is described in Sec. III.

Another mode used for measuring time-of-flight distributions is also indicated in Fig. 1. In this mode, a single-channel analyzer of variable channel

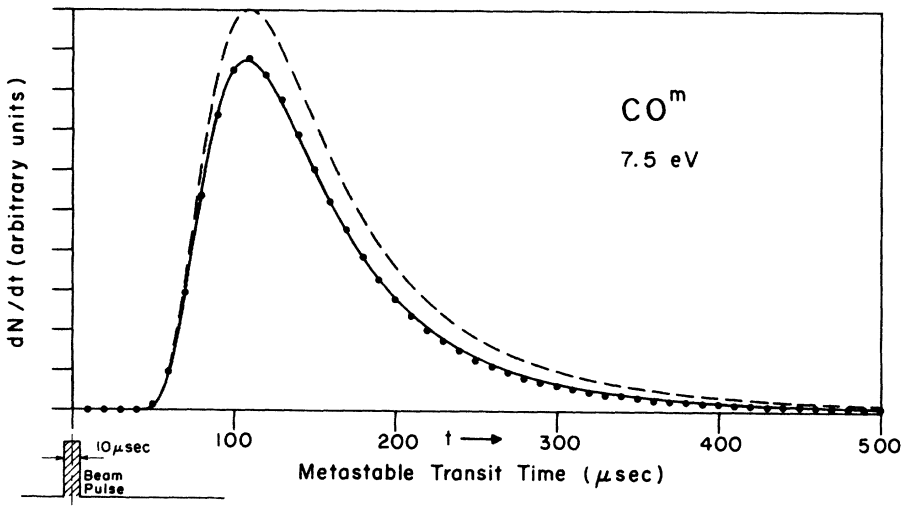

FIG. 3. Time-of-flight distribution of CO metastables in the $a^3\Pi$ state excited near the threshold of excitation. The solid line was fitted to the measured points by assuming a Maxwellian distribution containing a single metastable decay with a lifetime of $\tau = 800$ μsec. The dashed curve represents the pure Maxwellian without decay. Note that the solid curve shows a faster decline than the dashed curve because of metastable decay.

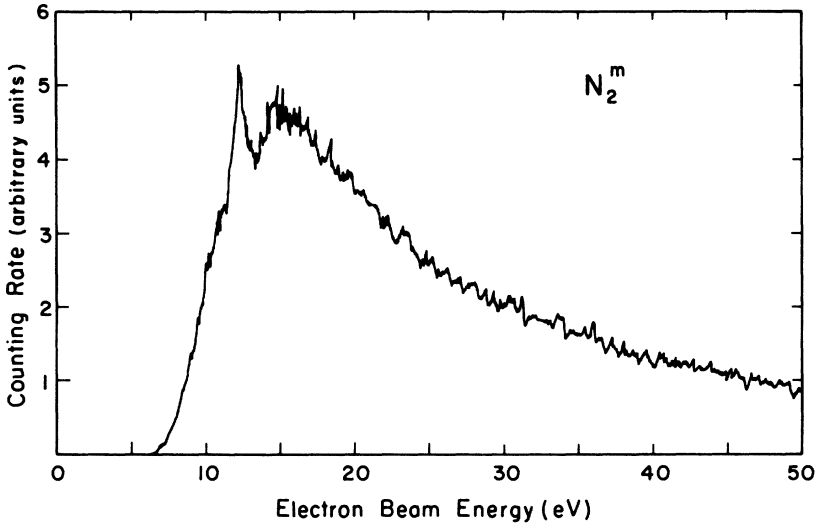

FIG. 4. Total metastable excitation function of N_2 using a Cu-Be surface in the metastable detector. At the lowest energies the signal is solely due to the $A^3\Sigma_u^+$ state. The sharp feature with a maximum at 12.2 eV is due to the $E^3\Sigma_g^+$ state. The $a^1\Pi_g$ state contributes for energies greater than about 9 eV. The photon component in the signal was completely eliminated by gating techniques (see text).

width and position was constructed. Its components, consisting of gate generators for window position and width, coincidence unit, counter, and oscilloscope, are drawn with thin lines in Fig. 1. Time-of-flight distributions in this mode were traced by varying the window position between 0 and, say 1 msec after the beam pulse. The two modes of operation just described yielded indentical time-of-flight distributions. The multiscaling method was used almost exclusively. In this mode apparatus drifts were negligible, statistics were better, and data were taken automatically. In contrast to this, in the single-channel method the signals had to be read off a counter and the operation in tracing time-of-flight distributions was largely manual and cumbersome.

However, the latter method enabled one to measure metastable excitation functions. To this end a ratemeter (not shown) was connected to the output of the coincidence unit parallel to the counter. The ratemeter output was applied to the Y deflection of another X-Y recorder (not shown) and the electron energy (X axis) was varied. Total metastable excitation functions are shown in Figs. 4 and 5. The photon component in the excitation functions, as well as metastable atoms produced by dissociative excitation,[5] was completely eliminated by the proper choice of counting-window width and position.

III. DATA EVALUATION AND RESULTS

The effective lifetimes of metastable N_2 and CO molecules were deduced from measured time-of-flight distributions such as shown in Figs. 2 and 3. The data reduction in the case of CO made use of that for N_2. Both cases are discussed separatively in Secs. III A and III B.

A. Nitrogen

1. $a^1\Pi_g$ State

In the case of the $A^3\Sigma_u^+$ state of N_2, metastable

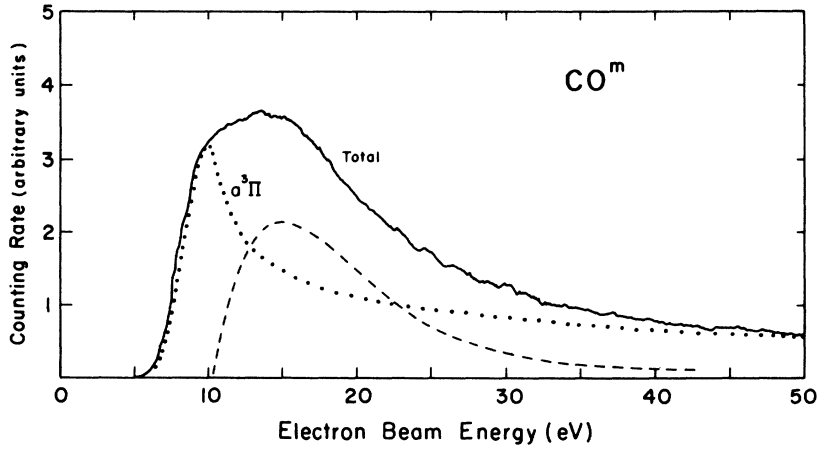

FIG. 5. Total metastable excitation function of CO excluding photons. Only the $a^3\Pi$ state contributes to our curve at the lowest energies. Ajello's excitation function of the $a^3\Pi$ state (dotted line) was normalized to ours in slope and substracted. The resulting curve (dashed line) represent the contribution of higher-lying state(s).

molecules traveled from the collision chamber to the detector without decay because of the long lifetime ($\tau \simeq 2$ sec) for this state.[6] Let us denote the velocity distribution of metastables in the $A^3\Sigma_u^+$ state by $D(v)$. Then in the simplest case of a completely diffuse-gas source and negligible momentum recoil of metastables after the electron collision, the distribution $D(v)$ is purely Maxwellian and given by

$$D(v)\,dv = A\,v^2 e^{-mv^2/2kT}\,dv\ , \tag{1}$$

where A is a normalization constant, m is the mass of N_2 molecules, and T is the temperature of the gas in the collision chamber ($T \simeq 293\,^\circ$K). The time-of-flight distribution is obtained from the velocity distribution by substituting $v = l/t$, where l is the distance between the collision chamber and detector ($l \simeq 6.4$ cm). The time-of-flight distribution corresponding to Eq. (1) is thus given by

$$S(t)\,dt = C(1/t^4)\,e^{-\beta/t^2}\,dt\ , \tag{2}$$

where $\beta = ml^2/2kT$ and C is another normalization constant. The functional form (2) represents the measurements quite well. This is seen in Fig. 2, where a Maxwellian distribution (solid line) [given by Eq. (2)] was fitted to the 8-eV data, which contained only metastables in the $A^3\Sigma_u^+$ state. The parameters in the least-mean-square fit were C and β. The value for β deduced from this fit agreed within a few percent with that calculated directly from $\beta = ml^2/2kT = 2.4\times10^{-8}$ sec^2. The quality of the fit in Fig. 2 shows that the assumptions of a diffuse-gas source and negligible momentum recoil are indeed approximately correct. Momentum-recoil effects are estimated in Appendix A. The slight discrepancy between the fitted curve in Fig. 2 and the measured points for the long transit times may have been due to the incomplete diffusiveness of the gas source.[7] It was further assumed that the reflection of metastables from the walls of the collision chamber produced negligible effects. In fact, we have never observed the survival of metastables after reflection from the metal walls of the collision chamber. It seems that most metastables become deexcited upon interaction with the metal walls whether or not secondary electrons are ejected.[3] Detailed knowledge of the functional form of the time-of-flight distribution such as Eq. (2) was not needed since the measured distribution for metastables in the $A^3\Sigma_u^+$ state could be utilized as a normalizing function. Let us first denote this normalizing function by $F(t)$, keeping in mind that it is approximately given by Eq. (2). The function $F(t)$ does not include terms accounting for the decay of the metastable molecules in transit and it is approximately equivalent to the velocity distribution (1). $F(t)$ will henceforth be referred to as the "velocity-dependent part" of the measured time-of-flight distributions.

A certain fraction of metastables decays in flight before reaching the detector if the metastable lifetime is of the order of the transit time to the detector. The measured time-of-flight distribution for a single metastable species decaying with a lifetime τ is then given by

$$S_\tau(t) = F(t)e^{-t/\tau}\ . \tag{3}$$

In this equation we have assumed that uv photons from decaying metastables on their way to the detector can be neglected. It is shown in Appendix B that this is indeed a good assumption under most conditions.

The measured time-of-flight distributions for N_2 above 9 eV contained two or three metastable species whose potential curves are drawn in Fig. 6. For most energies two metastable species were present and the time-of-flight distributions could be represented by

$$S_\tau(t) = F(t)(K_1 + K_2 e^{-t/\tau_2})\ , \tag{4}$$

where the constants K_1 and K_2 are a measure of the relative fractions of metastables in the two contributing states, the first being the $A^3\Sigma_u^+$ and the second the $a^1\Pi_g$ state.

In order to extract lifetimes from the data, the velocity-dependent part $F(t)$ in Eq. (4) was assumed to be given by the measured time-of-flight distribution of $A^3\Sigma_u^+$ metastables at 8 eV (Fig. 2) and was divided out. An example of the remaining metastable decay function

$$T(t) = K_1 + K_2 e^{-t/\tau_2} \tag{5}$$

is plotted in Fig. 7 for an electron energy of 13.5 eV. It is seen that the decay function reaches a

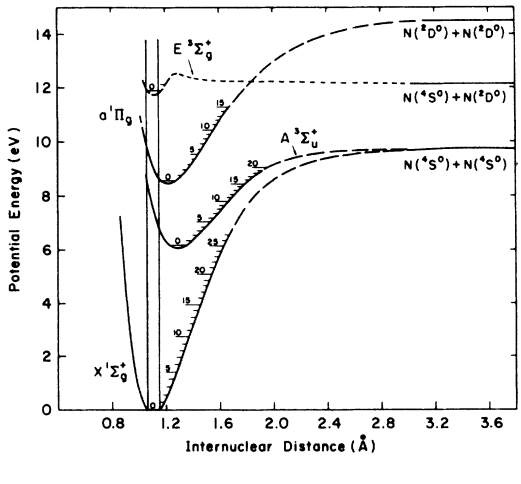

FIG. 6. Potential energy curves of ground state and important metastable states of N_2 (Ref. 8). Possible cascading to these states is not shown. The Franck-Condon region is indicated by vertical lines.

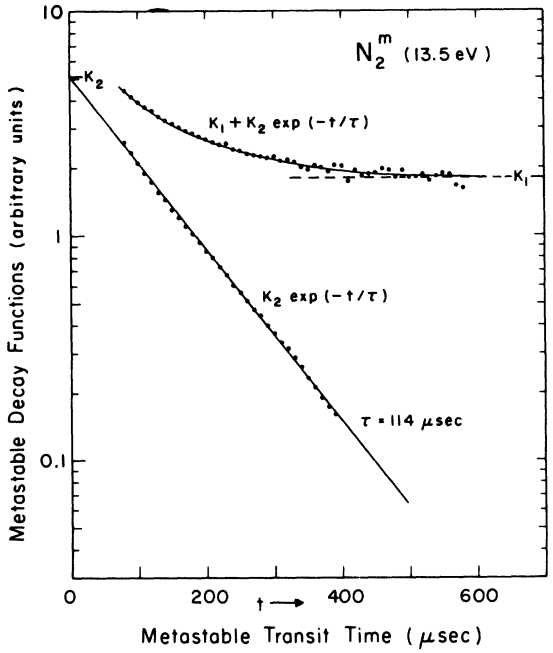

FIG. 7. Metastable N_2 decay function at 13.5 eV. After subtraction of the constant K_1 representing the contribution of the $A^3\Sigma_u^+$ state, one obtains a single metastable decay with $\tau = 114$ μsec due to the $a^1\Pi_g$ state. The solid curve through the data was calculated (see text).

constant value K_1 for long transit times. After substraction of K_1, a single exponential decay with a lifetime of $\tau = 114$ μsec remained. The constant K_2 was then determined by extrapolating to $t = 0$. The solid curve through the data points in Fig. 7 was calculated by inserting the values for K_1, K_2, and τ_2 into the decay function (5). The solid curve fitted to the time-of-flight distribution at 13.5 eV in Fig. 2 was also calculated by using the above values for K_1, K_2, and τ_2 together with the functional form (4), in which a Maxwellian distribution was assumed for the velocity-dependent part $F(t)$. This Maxwellian part was obtained from the 8-eV data in Fig. 2 by a least-mean-square fit. It is to be noted that the function $F(t)$ contains a normalization constant and only the ratio K_2/K_1 is of significance.

TABLE I. Lifetime for the $a^1\Pi_g$ state at various electron energies.[a]

E(eV)	τ (μsec)
10.5	121
11.5	117
12.2 (peak)	"154"
13.5	114
14.5	115

[a]The "lifetime" at 12.2 eV is a composite of the lifetimes of the $a^1\Pi_g$ and $E^3\Sigma_g^+$ states (see text).

Decay functions similar to those in Fig. 7 were obtained for various electron energies. Values for the lifetime τ_2 deduced at different electron energies are listed in Table I. It is seen that they agree well with each other. We adopt a value of 115 μsec for the lifetime τ_2 with a possible error of 20 μsec.

The ratio K_2/K_1 of the constants in Eqs. (4) and (5) is plotted in Fig. 8 as a function of electron energy. A smooth curve drawn through the data approached the energy axis near 9 eV. This energy agrees with the excitation threshold of the $a^1\Pi_g$ state in the Franck-Condon region of N_2 (see Fig. 6). This threshold value of about 9 eV together with the observed single exponential decay of lifetime τ_2 suggests that the decay was mainly due to metastables in the $a^1\Pi_g$ state.

2. $E^3\Sigma_g^+$ State

The sharp feature in the total-metastable-excitation function of N_2 (Fig. 4) at 12.2 eV was caused by metastables in the $E^3\Sigma_g^+$ state.[9] The energy resolution of the present apparatus was sufficiently high to clearly observe the E state and determine its lifetime. To this end, the time-of-flight distribution of N_2 metastables was measured at the 12.2-eV peak. In a preliminary reduction of the 12.2-eV data assuming two metastable species as before, a "composite" lifetime of 154 μsec was found. This was far greater than the lifetimes obtained at the higher as well as the lower energies (see Table I) and showed that a third metastable state was present with a lifetime larger than 154 μsec. The corresponding time-of-flight distribution is given by

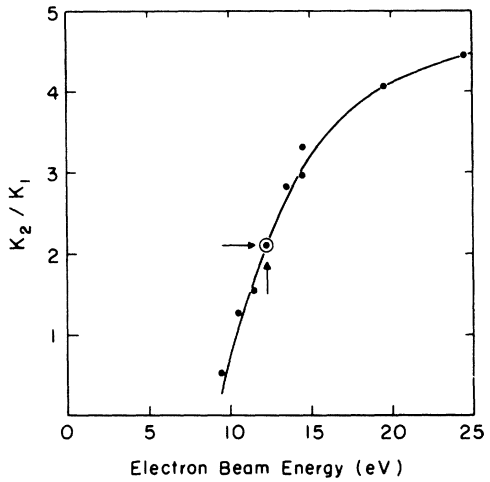

FIG. 8. The ratio K_2/K_1 which is a measure of the relative contribution of metastables in the $a^1\Pi_g$ and $A^3\Sigma_u^+$ states plotted as a function of electron energy. The ratio was obtained from graphs similar to Fig. 7. The interpolation at 12.23 eV (E peak) was used in the lifetime determination of the E state.

$$S_\tau(t) = F(t)(K_1 + K_2 e^{-t/\tau_2} + K_3 e^{-t/\tau_3}) , \quad (6)$$

where the constant K_3 is a measure of the fraction of metastables in the E state and τ_3 is its lifetime. The decay function

$$T(t) = K_1 + K_2 e^{-t/\tau_2} + K_3 e^{-t/\tau_3} \quad (7)$$

was obtained by dividing out the velocity-dependent part $F(t)$, for which the 8-eV time-of-flight data (Fig. 2) were used as before. The resulting function is plotted in Fig. 9. Clearly, it would be too ambiguous to determine all five parameters K_1, K_2, K_3, τ_2, and τ_3 from the 12.2-eV data alone. Therefore the lifetime τ_3 was deduced in the following way: The constant K_1 was obtained from Fig. 9 as indicated. A value of 2.1 was obtained for the ratio K_2/K_1 from an interpolation at 12.23 eV in Fig. 8. Thus K_2 was known. The factor $K_1 + K_2 e^{-t/\tau_2}$ was then calculated at 12.2 eV using $\tau_2 = 114$ μsec and subtracted from the decay function (7). It is seen in Fig. 9 that the resulting points follow a single exponential decay $K_3 e^{-t/\tau_3}$ with a lifetime of 190 μsec for the E state. The uncertainty in this value is about 30 μsec. The constant K_3 was obtained by extrapolating to $t = 0$. Having thus determined the parameters K_1, K_2, K_3, τ_2, and τ_3, the decay function (7) was calculated; it fits the data points in Fig. 9 quite well.

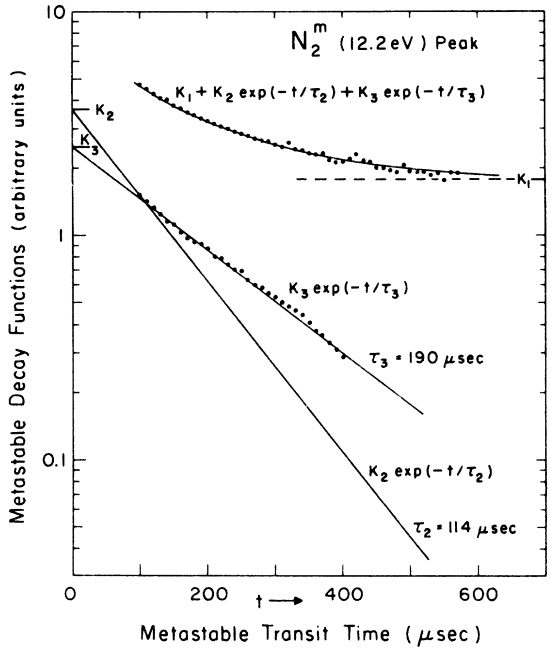

FIG. 9. Metastable N_2 decay function obtained at the 12.2-eV peak in the excitation function Fig. 4. The decay function contains three components due to the $A^3\Sigma_u^+$, $a^1\Pi_g$, and $E^3\Sigma_g^+$ states. The solid curve through the data was calculated (see text).

B. Carbon Monoxide

The method used in determining the lifetimes of CO metastables was essentially the same as that described above for N_2. The electron energy of 7.5 eV chosen in the measurements (Fig. 3) was close to the threshold of excitation of the $a^3\Pi$ state, as can be seen in Figs. 10 and 5. The time-of-flight distribution was again given by Eq. (3) which is appropriate for a single metastable decay. For the part $F(t)$ in Eq. (3), the time-of-flight distribution of N_2 at 7.5 eV was used (which was similar to that at 8 eV in Fig. 2). It could be assumed that the function $F(t)$ was the same for N_2 and CO because of the same masses of these molecules and negligible recoil. Again, as in the case of N_2, the details of the scattering process such as angular distributions did not need to be known.

The decay function $e^{-t/\tau}$ obtained from the CO and N_2 measurements at 7.5 eV is plotted in Fig. 11. The data points follow a decay with a lifetime of about 800 μsec for the $a^3\Pi$ state of CO. The solid curve in Fig. 3 was calculated using this lifetime and a Maxwellian distribution (2) for the function $F(t)$ in Eq. (3) with the same β as for N_2. The fit to the data in Fig. 3 is quite good. It is interesting to note than an even better fit was obtained with a lifetime of about 600 μsec. However, this is not necessarily a better value for the lifetime. A shorter lifetime merely compensates for the somewhat too slow decline of the pure Maxwellian (2) as compared with the actual time-of-flight distribution without decay.[7] It is easy to see that there is a correlation between the lifetime τ, the parameter β, and the power of t in front of the exponential in the time-of-flight distribution

$$S_\tau(t)\,dt = C(1/t^4)\, e^{-\beta/t^2} e^{-t/\tau}\, dt , \quad (8)$$

which was used to calculate to solid curve in Fig. 3. Therefore the procedure adopted in obtaining lifetimes from decay functions alone (Figs. 7, 8, and 11), *not* resorting to an explicit functional form such as Eq. (8) was judged more reliable despite the fact that Eq. (8) is a good approximation. The uncertainty in the CO lifetimes obtained from various runs was about 400 μsec. We adopt an average value of 1000 ± 400 μsec for the lifetime of CO metastables in the $a^3\Pi$ state as excited by 7.5-eV electrons at room temperature. It is to be noted that the $a^3\Pi$ state may not have a single lifetime.[6] Clearly our method did not allow us to investigate individual rotational and vibrational levels. We were able, however, to observe the $a^3\Pi$ state alone by choosing low enough electron energies and we always found a decay of these metastables with a lifetime of about 1 msec. This value has to be considered as the average for all vibrational and rotational levels of the $a^3\Pi$ state excited at 7.5 eV at room temperature.

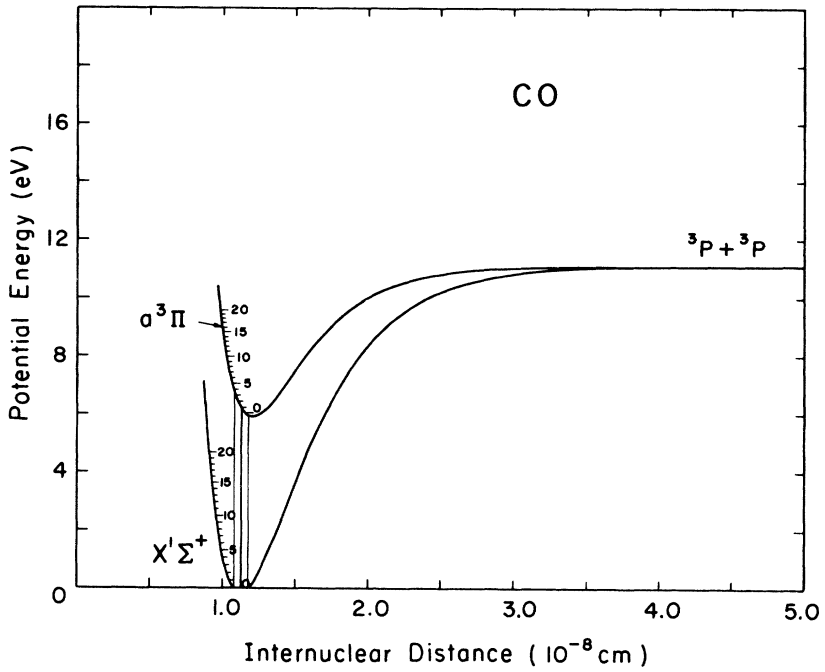

FIG. 10. Potential energy curves of ground and first excited state of CO. The Franck-Condon region is indicated by vertical lines. The curves were calculated assuming Morse potential functions. The parameters used for the ground state were $D_0 = 11.24$ eV, $\omega_e = 2169.52$ cm^{-1}, $\omega_e x_e = 13.45$ cm^{-1}, $r_e = 1.1282$ Å, $T_e = 0$. The parameters used for the metastable $a^3\Pi$ state were $D_0 = 5.18$ eV, $\omega_e = 1739.25$ cm^{-1}, $\omega_e x_e = 14.47$ cm^{-1}, $r_e = 1.2093$ Å, $T_e = 6.057$ eV.

At higher electron energies the measured lifetime of CO metastables was about 150 μsec and thus markedly shorter than that for the $a^3\Pi$ state excited by 7.5-eV electrons. There is, therefore, strong evidence that above 10 eV another higher-lying state contributed. This fact is further corroborated by the shape of the excitation function in Fig. 5. The excitation function of the higher-lying state alone was obtained by normalizing Ajello's excitation function for the $a^3\Pi$ state[10] to ours at the lowest energies and subtracting it from our total-excitation function. The onset of the resulting excitation function is near 10.4 eV. The unknown state in question cannot be a known singlet state because all singlet states in this energy range have allowed transitions to lower states. It is conceivable that higher vibrational levels of the $a^3\Pi$ state are populated in cascading transitions for electron energies above 10 eV and that these levels have shorter lifetimes. On the basis of selection rules it seems unlikely that the known higher-lying triplet states of CO are metastable.

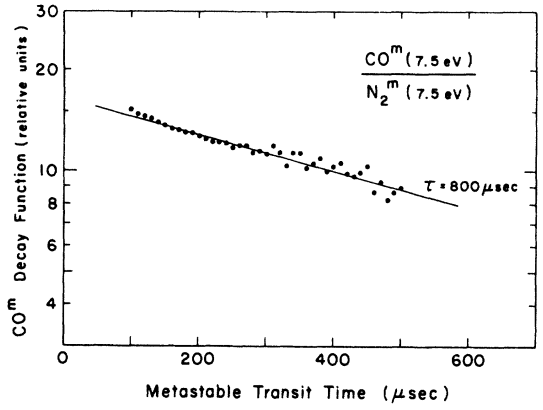

FIG. 11. Metastable CO decay function which was determined by dividing the CO time-of-flight data (Fig. 3) by those for N_2 at 7.5 eV.

Since the determination of lifetimes of the order of 1 msec or longer is difficult under most circumstances, we performed an additional consistency check of our method by estimating the lifetime of He metastables in the 2^1S_0 state. As a result[11] we obtained a lifetime of $\gtrsim 10$ msec for this state. This value is, of course, a preliminary one. However, from measurements such as that in He we feel that our method is capable of yielding reliable lifetimes at least into the 10-msec domain.

A summary of our lifetime measurements is presented in Table II.

IV. DISCUSSION AND CONCLUSION

In this section we further discuss our results and compare them with other available data.

Our lifetime value of 115 ± 20 μsec for the $a^1\Pi_g$ state of N_2 is in excellent agreement with a value of 120 ± 50 μsec determined by Olmsted *et al.*[12] in a time-of-flight experiment. The uncertainty in Olm-

TABLE II. Measured lifetimes of N_2 and CO metastables.

State	τ (μsec)
$N_2(a^1\Pi_g)$	115 ± 20
$N_2(E^3\Sigma_g^+)$	190 ± 30
$CO(a^3\Pi)$	1000 ± 400
CO(?)	150

sted's value, however, is considerably larger than ours. There is also reasonable agreement with Lichten's value of 170 ± 30 μsec which was obtained in an experiment in which the distance between detector and excitation region was varied.[13] Our lifetime for the $a^1\Pi_g$ state further agrees well with Shemansky's measurements involving optical-absorption techniques.[14] Shemansky finds that the lifetimes calculated from his measurements increase slowly from 140 μsec for the $\nu' = 0$ level to 160 μsec for the $\nu' = 8$ level with a probable error of about 30%. Since we cannot distinguish individual vibrational levels, our measured lifetimes are the average over all contributing levels. It can be seen from Fig. 6 that levels around the $\nu' = 3$ level are preferentially excited in Franck-Condon transitions. According to a table given by Shemansky,[14] this corresponds to a lifetime of about 150 μsec. The agreement between Shemansky's and our results is very good, especially in view of the fact that Shemansky's values should be considered an upper limit.[15] Holland[16] and Jeunehomme[17] have reported lifetimes of 80 and 10 μsec, respectively, for the transition $a^1\Pi_g - X^1\Sigma_g^+$. These lifetimes, in particular the latter one, appear to be too short. The reason for the discrepancy is not clear.

The lifetime of 190 ± 30 μsec for the $E^3\Sigma_g^+$ state of N_2 can be compared with Freund's[18] estimate of 270 ± 100 μsec. In arriving at his value, Freund assumed a lifetime of 60 msec for the $a^3\Pi$ state of CO and measured the difference in transition probabilities of the $E^3\Sigma_g^+$ state of N_2 and the $a^3\Pi$ state of CO. However, a lifetime of 60 msec for the $a^3\Pi$ state of CO appears to be rather unrealistic. If we use our measured lifetime of 1 msec for this state, we deduce a lifetime of about 210 μsec for the $E^3\Sigma_g^+$ state using Freund's data. This is in much better agreement with our result for the $E^3\Sigma_g^+$ state.

There have been a few attempts to measure the lifetime of the $a^3\Pi$ state of CO which resulted in large discrepancies. By varying the position of his metastable detector, Papaliolios[19] found a lifetime of 60 msec, which is almost two orders of magnitude larger than our value. On the other hand, Hansche[20] determined a lifetime of 10 μsec. It is doubtful indeed whether Hansche observed the pure radiative decay of metastables in the $a^3\Pi$ state and whether Papaliolios observed radiation from the $a^3\Pi$ state at all. Donovan and Husain[21] quote a radiative lifetime of 12 msec and find this consistent with their measurements inasmuch as they could not see any emission (Cameron bands) from the $a^3\Pi$ state to the $X^1\Sigma^+$ ground state. In contrast to these results, Olmstead *et al.*[12] could not observe the $a^3\Pi$ state in their time-of-flight study because this state was claimed to be too short lived and therefore metastables decayed before reaching their detector. They found their observations to be consistent with Hansche's lifetime of 10 μsec. It is interesting to note that in Olmsted's as well as in our measurements, the distance between detector and excitation region was almost the same. In our case, however, it was a relatively simple matter to clearly observe the $a^3\Pi$ state. This indicates that the lifetime involved must be much larger than 10 μsec.

Our measured lifetime of 1 msec is consistent with Ajello's[10] excitation cross-section measurements for the $a^3\Pi$ state. Assuming a radiative lifetime of 1 msec, Ajello finds a maximum cross section of about 1×10^{-16} cm^2 at an electron energy of about 10 eV. This cross section equals that for the $A^3\Sigma_u^+$ state of N_2 within an order of magnitude as is to be expected.[10] Therefore the lifetime of the $a^3\Pi$ state should be expected to have a value of about 1 msec.

Owing to the marked decrease in CO metastable lifetimes from 1 to about 0.15 msec at energies above that required for the direct excitation of the $a^3\Pi$ state, it appears likely that higher-lying states contributed. Although the onset for these states at 10.4 eV (Fig. 5) agrees with the excitation energy of the $b^3\Sigma^+$ state it seems unlikely that this state could be detected in our experiment in view of its short radiative lifetime of about 10^{-7} sec.[22] It is interesting to note that Olmsted *et al.*[12] detected a metastable state in CO with a threshold at 10.5 eV and a lifetime of the order of 0.1 msec. This is in complete agreement with our observations. These authors suggested that the $b^3\Sigma^+$ state may be the state in question. This explanation is not valid if the lifetime of this state is indeed 10^{-7} sec.[22] In a further check, the metastable detector distance was increased from 6.4 to 21 cm. This resulted in an excitation function more similar to that of Ajello for the $a^3\Pi$ state in Fig. 5. The maximum in the original total excitation function at 14 eV (Fig. 5) now appeared only as small structure, indicating again a lifetime of about 0.1 msec for the unknown metastable state(s). In any case, the situation at energies above that for the direct excitation of the $a^3\Pi$ state is rather complex. We have therefore performed our lifetime measurements of the $a^3\Pi$ state of CO very close to threshold in order to eliminate completely effects due to higher-lying states.

ACKNOWLEDGMENTS

We wish to thank A. G. Haas and E. W. Erdman for their most helpful assistance in the data analysis and Dr. W. C. Wells for useful discussions.

APPENDIX A: METASTABLE RECOIL EFFECTS

The measured time-of-flight distributions were Maxwellian (with or without decay) to a good degree of accuracy as is seen in Figs. 2 and 3. Although we made no use of any analytic form for the time-of-flight distributions in obtaining lifetimes, it is interesting to examine recoil effects and see why they are rather negligible. For a diffuse-gas source in which gas enters the electron beam uniformly from all directions, the velocity distribution function is given by[23]

$$f(v)dv = A\, v^2\, e^{-\alpha(B^2+U^2)}\, \frac{\sinh 2\alpha BU}{2\alpha BU}\, dv\ , \tag{9}$$

where A is a constant, $\alpha = M/2kT$, and the quantities B and U are given by

$$B^2 = v^2 + (m/M)^2 u_0^2 - 2(m/M)u_0 v\cos\theta\ , \tag{10}$$

$$U^2 = 2(m/M^2)(\tfrac{1}{2} m u_0^2 - E^*)\ . \tag{11}$$

In Eqs. (10) and (11), m is the electron mass, M the molecular mass, u_0 the initial velocity of the electrons before the collision, E^* the excitation energy of the state in question, and θ the angle of observation ($\theta = 90°$).

In the derivation of Eq. (9), a Maxwellian ground-state gas before the collision and s-wave scattering were assumed. Equation (9) reduces to a purely Maxwellian distribution under our experimental conditions as follows: The electron energy $\frac{1}{2}m\mu_0^2$ before the collision did not exceed 15 eV in our lifetime measurements. Therefore Eq. (10) reduces to $B = v$, and further $\alpha U^2 < 1\times 10^{-2}$, and for transit times longer than about 100 μsec, $2\alpha BU \lesssim 0.2$. This finally yields $1.00 \lesssim \sinh(2\alpha BU)/2\alpha BU < 1.01$, and hence Eq. (9) becomes a Maxwellian distribution function. The finite detector solid angle resulted in a spread in the angle θ around the value $\theta = 90°$. It is readily estimated from Eqs. (9) and (10) that this also caused a negligible effect.

APPENDIX B: uv PHOTONS FROM METASTABLE DECAY

As seen from the time-of-flight distribution in Figs. 2 and 3, there was no photon background for transit times shorter than about 50 μsec, i.e., photons from metastables decaying far enough away from the detector caused no measurable signal. However, because of the large increase in solid angle near the detector, the possibility of a small photon contribution existed for the longer transit times. Let us now examine the photon background numerically.

At a fixed time t after the beam pulse, the *photon* counting rate is given by

$$C_p = B\frac{\gamma_p}{\tau}\, e^{-t/\tau}\int_0^{l/t} \frac{\Omega(v,\, t)}{4\pi}\, v^2 e^{-\alpha v^2}\, dv\ , \tag{12}$$

where the constant B is a measure of the total number of metastables per beam pulse that move towards the detector, γ_p is the photoelectric yield, τ the lifetime of the metastables in question, l the distance between excitation region and detector, $\alpha = M/2kT$, and $\Omega(v,\, t)$ is the solid angle subtended by the detector as seen by metastables of velocity v at a point $(l - vt)$ away from the detector. It has been assumed in Eq. (12) that photons are emitted isotropically in all directions. For a detector with a circular aperture of radius r, the solid angle is given by

$$\Omega(v,\, t) = 2\pi\left(1 - \frac{l - vt}{[(l-vt)^2 + r^2]^{1/2}}\right)\ . \tag{13}$$

According to Eqs. (1)–(3), the *metastable* counting rate for a single metastable decay is given by

$$C_m = B\gamma_m\, e^{-t/\tau}(l^3/t^4)\, e^{-\alpha l^2/t^2}\ , \tag{14}$$

where γ_m is the secondary electron yield for the metastables in question. In comparing metastable and photon signals, we are interested in the number of metastables which have decayed during their flight to the detector [rather than the total number of metastables given by Eq. (14)]. The resulting difference in metastable counting rate is given by

$$\Delta C_m = B\gamma_m(1 - e^{-t/\tau})\,(l^3/t^4) e^{-\alpha l^2/t^2}\ . \tag{15}$$

Combining Eq. (12), (13), and (15) yields the ratio

$$R(t) = \frac{C_p}{\Delta C_m} = \frac{\gamma_p}{2\gamma_m}\,\frac{t/\tau}{e^{t/\tau} - 1}\left(\frac{l}{l}\right)^3 e^{\alpha l^2/t^2} \times\int_0^{l/t}\left(1 - \frac{l - vt}{[(l-vt)^2 + r^2]^{1/2}}\right) v^2 e^{-\alpha v^2}\, dv \tag{16}$$

for the relative photon background as a function of time. A detailed analysis of the above expression shows that for all transit times longer than 100 μsec, the ratio R has an upper limit of

$$R < 0.1\,(\gamma_p/\gamma_m)\ . \tag{17}$$

The ratio of photoelectric to secondary electron yield is probably of the order of 0.1 or less for the energy of about 6 eV involved[24] in the excitation of the $a^3\Pi$ state of CO. This amounts to a photon contribution of less than 1% as compared to the change in metastable signal due to metastable decay. Thus the measured lifetime of the $a^3\Pi$ state of CO was not affected by any photon background.

In the case of N_2, the excitation energies involved are of the order of 10 eV. In this energy range, the

yields γ_p and γ_m may be comparable,[24] although γ_p is still likely to be smaller than γ_m. Hence in the worst case, the ratio R could approach a value of 10%. This would increase our lifetime values for N_2 by about 5%, as a discussion of Eq. (16) shows. However, this error is small compared with the uncertainties originating from other sources.

It is interesting to note that in the metastable decay functions (Figs. 7, 9, and 11), an upward curvature deviating from the linearity in the semilog plots was observed for transit times below 100 μsec. This is completely consistent with Eq. (16).

*Work supported in part by the National Aeronautics and Space Administration (NGL-39-011-030) and by the Advanced Research Project Agency (DA-31-124-ARO-D-440).

†Present address: Dept. of Physics, Southern Illinois University, Carbondale, Ill. 62901.

[1]W. L. Borst, Phys. Rev. 181, 257 (1969).

[2]Since our interest was chiefly in lifetime measurements, possible small secondary effects due to magnetic collimation were not investigated in detail. It was ascertained by proper collection of electrons and low gas pressures that secondary effects in the energy range from 5 to 50 eV were negligible. At higher energies, however, we have found that electrostatically focused electron guns yield more accurate cross sections. [See W. L. Borst and E. C. Zipf, Phys. Rev. A 1, 834 (1970); 1, 1410 (1970)].

[3]H. D. Hagstrum, Phys. Rev. 96, 336 (1954).

[4]P. J. MacVicar-Whelan and W. L. Borst, Phys. Rev. A 1, 314 (1970).

[5]W. L. Borst and E. C. Zipf (unpublished).

[6]D. E. Shemansky, J. Chem. Phys. 51, 689 (1969).

[7]Note that for an ideal-gas *beam*, the transit time occurs as t^{-5} in front of the exponential factor in Eq. (2) instead of t^{-4} for a diffuse-gas source. It was found in the present measurements that a factor $t^{-4.1}$ would yield even better agreement with the data points than the factor t^{-4} used in the calculation of the solid curves in Fig. 2. However, as described in the text, there was no need for an accurate analytic expression for the time-of-flight distributions.

[8]F. R. Gilmore, Rand Corp. Report No. RM-4034-PR 1964 (unpublished).

[9]The calibration of the energy scale in Fig. 4 was obtained by positioning the sharp maximum in Fig. 4 at an energy of 12.23 eV [See H. Ehrhardt and K. Willmann, Z. Physik 204, 462 (1967)]. The required shift in energy scale was of the order of 0.1 eV.

[10]J. Ajello (private communication).

[11]W. L. Borst and E. C. Zipf, Abstracts of Papers, Twenty-third Gaseous Electronics Conference, Hartford, 1967 (unpublished).

[12]J. Olmsted III, A. S. Newton, and K. Street, J. Chem. Phys. 42, 2321 (1965).

[13]William Lichten, J. Chem. Phys. 26, 306 (1957).

[14]D. E. Shemansky, J. Chem. Phys. 51, 5487 (1969).

[15]D. E. Shemansky (private communication).

[16]R. F. Holland, J. Chem. Phys. 51, 3940 (1969).

[17]M. L. Jeunehomme, Air Force Weapons Lab. Report No. AFWL-TR-66-143, 1967 (unpublished).

[18]Robert S. Freund, J. Chem. Phys. 50, 3734 (1969).

[19]C. Papaliolios, Ph. D. thesis, Harvard University, Cambridge, Mass., 1965 (unpublished).

[20]G. E. Hansche, Phys. Rev. 57, 289 (1940).

[21]R. J. Donovan and D. Husain, Trans. Faraday Soc. 63, 2879 (1967).

[22]R. P. Schwenker, J. Chem. Phys. 42, 1895 (1965).

[23]J. C. Pearl, D. P. Donelly, and J. C. Zorn, in *Sixth International Conference on the Physics of Electronic and Atomic Collisions, Abstract of Papers*, edited by I. Amdur (MIT Press, Cambridge, Mass., 1969), p. 240.

[24]W. L. Borst, Ph. D. thesis, University of California, Berkeley, 1968 (unpublished).